Computer-aided design of doped oxide catalysts

Raj Ganesh S. Pala

Abstract | An elementary overview of density functional theory and its application to computational catalyst design is presented. The central concepts like reactivity descriptor, Bronsted–Evans–Polanyi relationship, Sabatier principle and electronic structure factors that have enabled successful design of transition metal alloy surfaces as catalysts for relatively simple reaction systems are discussed. Extension of these concepts to the design of doped oxide catalysts is addressed. A viewpoint on the design of doped oxide catalysts as single site heterogeneous catalysts is provided. The case study presented in the design of doped oxide catalysts illustrates the synergism between experiments and computer aided catalysts design. Here, using doped oxide catalysts, mechanisms of non-and pseudo-Mars and Van Krevelen in heterogeneous catalytic oxidation were unraveled.

1. Preamble and introduction

This review is aimed at the experimental catalytic chemists, chemical and materials engineers and theory students who are beginning their research in computational modeling and design of heterogeneous catalysts and solid state surfaces. An attempt has been made to elucidate the key qualitative ideas behind the computational methodology while references to more elaborate discussions have also been provided. In order to keep this review concise, the examples and references discussed here are more illustrative than comprehensive. We restrict this review to computational studies that aim at using density functional theory as a design and predictive tool in catalyst discovery. While this limits the scope of this review, it is also indicative of the excitement of this field in realizing the dreams of computational catalyst design. It is also goes without saying that the computational design strategies have to be judiciously combined with experiments to utilize both the experimental and simulation tools to their complete potential.

Heterogeneous catalysis not only involves heterogeneity in terms of phases of the reactants/products and the catalysts, but also heterogeneity in terms of the chemically active sites at the surface of the catalyst. The heterogeneity in chemically active sites can be present not only on the surface but also in the sub-surface region of the catalyst [1–3]. The presence of different catalytically active sites in the surface/sub-surface of the catalyst can couple the bond breaking step to other transport processes. This suggests that the reactants can be activated or partially functionalized at a particular site, which may diffuse to another site where it may get functionalized further before diffusing to another site from where it may get desorbed. Such processes, while making experimental characterization difficult, enhance the diversity and enrich the phenomenology of the heterogeneous catalytic system.

The variety in catalytically active sites introduces diversity in the types of chemical reactions that take place and hence, the selectivity of the heterogeneous catalytic processes is not 100%. This is in contrast

Department of Chemical Engineering, Indian Institute of Technology, Kanpur 208 016, India
rpala@iitk.ac.in

to a homogeneous catalytic system in which the catalytically active site is unique and hence, the selectivity of these processes is very high. Attempts are being made to introduce an unique and structurally uniform catalytically active site in a heterogeneous catalytic system and such a catalyst is called a single site heterogeneous catalyst (SSHC) [3].

One of the "simplest" SSHC is doped oxide catalysts. In these catalysts, some of the cations in the surface of a host oxide M_mO_n are replaced by a different cation D (dopant), to form a single-phase doped oxide having the chemical formula $D_xM_{m-x}O_n$ and $(x/m-x) < 0.2$ [5–33]. Anion substitution is also possible, but these have been explored to a lesser extent [4]. The introduction of the substitutional dopant in the host oxide is aimed at generating a structurally well-defined catalytic active site centered on the dopant. Such attempts have a long history in catalysis and factors governing these catalysts have been published as early as 1968 [21], but with the introduction of modern experimental and computational tools of analysis, a greater insight has been obtained. If the dopants are precious metals, doped oxide catalysts offer significant advantages as very few precious metal atoms are utilized when compared to cluster of precious metal atoms supported on an oxide. Also, as the dopant is coordinated to the other atoms of the host oxide, the deactivation of the dopant by sintering is not expected to occur.

The atomic size of the catalytically active sites makes the experimental study of catalysis by doped oxides very challenging. While the experimental methods of preparation can in principle form doped oxides, other alternatives like a physical mixture of two oxides, or small oxide clusters of D supported on the oxide M_mO_n, or very small neutral clusters of the metal D supported on the oxide M_mO_n, or a doped oxide in which all dopant atoms are hidden in the bulk of the material are also possible. Further, the experimental study of the stability of doped oxides during reaction conditions and its possible transformation to any of the above mentioned chemical systems is also challenging. However, numerous experimental studies have addressed these issues and these studies are indicative of doped oxides being good catalysts for a variety of reactions [5–25].

The experimental studies have also been complemented by a significant number of quantum chemical computational studies [26–33]. In general, the compositional and structural complexity of working catalysts makes it difficult to unambiguously model the active sites. In this respect, the SSHC in general, specifically doped oxides, offer a significant advantage because of the size and structural "simplicity" of the catalytically active site. The overall goal of computational modeling is to not only serve as a *post-facto* tool for clarifying the working principles of existing catalysts, but to also serve as a *predictive tool in the discovery of new catalysts*.

Over the last decade, computational catalytic studies have resulted in the discovery of a variety of transition metal alloys that are good catalysts for a variety of important reactions, especially involving diatomic molecules [34]. The use of density functional simulations has not only reduced the amount of experimental labor involved in catalysts discovery, but they have also enlightened the scientific under pinning on what makes a good catalytic surface [3,34,35]. Many correlations like Bronsted–Evan–Polanyi relationship that emerged from empirical studies are better understood now as the electronic structure behind these correlations can be computed efficiently via density functional theory [36,37]. The scope of computational design is constantly being broadened to include more complex surfaces like oxides and sulfides and also to include more complex phenomena like electrochemical and photoelectrochemical bias and the effects of solvation [34]. Studies on doped oxide surfaces have identified new mechanisms over and above the traditional Mars and Van Krevelen mechanism which shows promise of new catalysts for important hydrocarbon reactions [29]. Most importantly, the author's experience on doped oxide catalyst design stresses the symbiosis that can exist in a closely coupled experimental–computational catalytic design effort.

2. Density functional theory: Context, pros and cons

A variety of computational methods are used in catalysis to capture the two central features of catalysis, namely, energetics of bond breaking and kinetic rate data. The latter in turn is quite important in the design and optimization of the chemical reactors. While all the relevant computational tools cannot be reviewed here, it is important to briefly state the context, power and limitations of density functional theory (DFT) compared to other methods.

2.1. *Physical models for catalytically active site in a surface*

The active site in a heterogeneous catalyst is part of the surface and hence, a realistic physical model of the active site necessitates representing a collection (roughly, at least a dozen) of atoms to compute the essential features of *surface reactivity*.

Figure 1: Two approaches to a physical model of a catalytic active site on a surface (Left) Embedded cluster: The reactant (R-R') and a small portion (red hemisphere) of the surface is modeled quantum chemically and the surrounding areas (green hemisphere) are modeled classically. (Right) Surface super-cell: All parts of the system are modeled quantum chemically. A two dimensional slab (red rectangular box) is used as a model for a semi-infinite surface. The two dimensional box is laterally translated and the size of each translation is indicated by a ⇔. Such a translation is called periodic boundary condition and ideally, the size of lateral translations should be such that there is negligible interaction between the reactants in one box with the reactants of the other box.

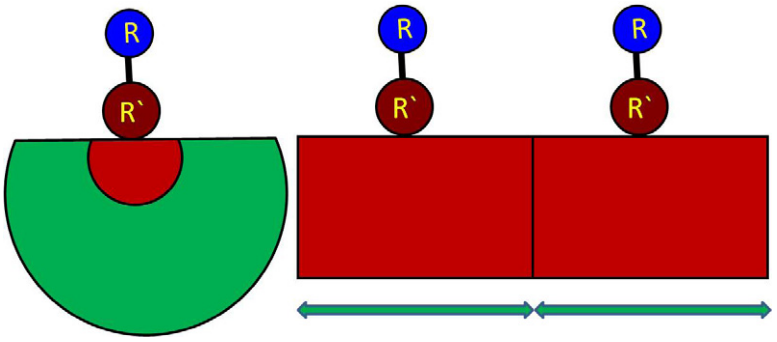

Treating a collection of atoms to capture surface reactivity makes the problem computationally demanding as compared to treating gas phase reactivity and a judicious choice has to be made between computational efficiency and accuracy. A method that is computationally very efficient, but whose accuracy requires extensive system-specific parameterization is the classical reactive force-field approach. In contrast to these methods, quantum chemical *ab-initio*/first principle methods do not require any system specific parameterization, but are computationally very demanding.

Two approaches have been developed in the context of representing the physical model of the surface: 1) Surface super-cell and 2) Embedded cluster (Fig. 1) [35]. In the surface super-cell approach, the surface is represented via a finite slab in which all the atoms are represented quantum chemically [35]. In the embedded cluster approach, only a small chemical cluster (comprised of approximately dozen atoms) is represented quantum chemically. The rest of the surface beyond this small cluster is represented via classical force-field that mainly provides the correct Madelung (or electrostatic field) to the cluster modeled quantum chemically [33,35,38]. The accuracy of both these approximations crucially depends upon the extent of the structural relaxation due to the creation of the surface or binding of reactant and products i.e., the more short-ranged the relaxations, the better is the approximation of representing a semi-infinite surface by a thin slab or by an embedded cluster. All the calculations discussed in this review have been performed using the surface super-cell approach.

Historically and culturally, these two approaches for representing catalysis at the surface reflect two different views of what the surface is. The chemists viewed the surface as a "giant molecule" comprising of atoms and atomic orbitals [39], hence, they played a greater role in developing the embedded cluster approach. The material physicists viewed the surface as an object resulting from the cleavage of a bulk crystal and hence, they played a greater role in developing the surface super-cell approach [37].

2.2. *Two complementary approaches to electronic structure: WFT and DFT*

The above two views are also reflected in the two complementary quantum chemical models used for obtaining computational results. The embedded cluster approach typically employs the wave function theory (WFT) to obtain the energetics and the surface super cell approach typically employs the density functional theory (DFT). It should also be noted that both the physical models (embedded cluster/surface unit cell) can be addressed using both the quantum chemical methods (WFT/DFT) [35].

A very good physical introduction to both the wave function and density functional method is provided in a recent text book "Quantum mechanics chemistry" by Jack Simons and Jeff Nichols (this text book can be accessed online at http://simons.hec.utah.edu/TheoryPage/BookPDF/TableofContents.html) [40]. A very comprehensive and advanced discussion of these methods is provided in the book "Molecular electronic structure theory" by T. Helgaker,

P. Jorgensen and J. Olsen [41]. The book "Electronic structure: Basic theory and practical methods" by R. Martin [42] provides a comprehensive introduction to density functional theory and simulations. A variety of methodological and practical issues associated with the WFT/DFT methods is also addressed in a very pedagogical manner by M. Springborg in "Methods of electronic-structure calculations: From molecules to solids" [43].

2.3. *A very brief overview of wave function theory*

Briefly, in the WFT approach [40], the wave function plays the central role in computing the energetics. The wave function is represented using a single Slater determinant or a sum of many Slater determinants and the wave function is obtained by solving the Schrodinger equation. The electrons of the surface and those belonging to the reactants bound to the surface reside in the "molecular orbitals" obtained from linear combination of atomic orbitals. The computation of such orbitals entails the calculation of the electronic structure of the system by essentially specifying the atomic number of atoms in the system and an initial guess for the positions of the atoms. Thus, the charge of the nuclei provides an *external* potential for the electrons within which the electronic structure is to be solved.

The quantum mechanical Hamiltonian that governs this system is:

$$\hat{H} = \hat{V}_{ex} + \hat{V}_{in} + \hat{T}_I + \hat{T}_e + E_{II} \tag{1}$$

where, $\hat{H}$ = Hamiltonian operator for the system; $\hat{V}_{ex}$ = External potential provided by the nuclei; $\hat{V}_{in}$ = Internal potential between the electrons; $\hat{T}_I$ = Sum of the kinetic energies of nuclei; $\hat{T}_e$ = Sum of the kinetic energies of the electrons; E_{II} = Classical electrostatic energy between the nuclei.

More explicitly, writing the full expression for the operators:

$$\hat{H} = \sum_{i,I} \frac{Z_I e^2}{|r_i - r_I|} + \sum_{i<j} \frac{e^2}{|r_i - r_j|} - \sum_I \frac{\hbar^2}{2m_I} \nabla_I^2 - \sum_I \frac{\hbar^2}{2m_e} \nabla_e^2 + \sum_{I<J} \frac{Z_I Z_J e^2}{|r_I - r_J|} \tag{2}$$

where, $\hbar = \frac{h}{2\pi}$; (where, h =Planck's constant); m_e, m_I = Electronic mass and nuclear mass of an element I, respectively; e, $Z_I e$ = Electronic charge and nuclear charge of a nucleus of atomic number Z_I, respectively; r_i, r_I = Position vector for an electron i and nucleus I, respectively.

As $\frac{m_e}{m_I} \sim 1/1840$, the motion of the electrons can be expected to be much faster than the motion of the nucleus. This makes it possible to decouple the electronic and nuclear motions leading to the Born-Oppenheimer approximation. Hence, the electronic structure is solved for a fixed position of the nucleus, which amounts to setting m_I to infinity and neglecting the kinetic energy of the nucleus. The expectation value for the total energy of the system is given by $E = \frac{\langle \psi | \hat{H} | \psi \rangle}{\langle \psi | \psi \rangle}$, where $|\psi\rangle$ is the many body wave-function of the system.

Advanced methods in wave function theory such as coupled cluster and many-body perturbation theories do give very accurate answers [40,41,43], but as the computational cost of these methods is high, only very small systems can be modeled. Further, the high computational cost of these advanced wave function methods restricts their use to very few calculations. However, as computational catalyst design involves modeling large systems [34,35] and performing numerous calculations, wave functional theory methods have not been used extensively and hence, have not been elaborated further in this review.

2.4. *Brief overview of density functional theory*

2.4.1. *Basis for DFT: Hohenberg-Kohn theorem*

In density functional theory [42], employed usually in the surface super-cell approach, the density of the electrons is the central quantity. The density of the electrons of the system can be obtained by the expectation value of the density operator:

$$\hat{n}(r) = \sum_{i=1,N} \delta(r - r_i); n(r) = \frac{\langle \psi | \hat{n}(r) | \psi \rangle}{\langle \psi | \psi \rangle} = N \frac{\int d^3 r_2 \ldots d^3 r_N |\psi(r, r_2, \ldots, r_N)|^2}{\int d^3 r_1 \ldots d^3 r_N |\psi(r_1, r_2, \ldots, r_N)|^2}. \tag{3}$$

Hohenberg-Kohn (HK) proved that there always exists an unique electron density corresponding to a given potential "external" to the electrons. This external potential can be due to the nucleus or any other source like an electric field external to the system of electrons and nuclei. As the Hamiltonian is completely defined with the specification of the external potential, it follows that the many-body wave function of the system can be associated with an unique ground state electron density. Since other properties like the internal and kinetic energy of the electrons can be expressed as an expectation value of the wave function, all such properties are uniquely determined by the ground state electron

density. Thus, the total energy of the system can be written as:

$$E_{HK}[n] = T[n]+E_{in}[n]+\int d^3rV_{ex}(r)n(r) +E_{II}=F_{HK}[n]+\int d^3rV_{ex}(r)n(r)+E_{II}. \quad (4)$$

The functional $F_{HK}[n]$ is a *universal* functional of electronic density in the sense that it independent of $V_{ex}(r)$ and the "chemical" nature of the system, and determines the potential and kinetic energies of the electrons. Thus, from eq. (4), it is clear that the exact ground state energy can be obtained at the variational minimum of $E_{HK}[n]$with respect to electronic density. However, HK theorem does not provide a recipe for determining the universal functional form of $F_{HK}[n]$. *In other words, even if we knew the ground state electron density, we still cannot partition the energies into kinetic and potential energies.*

2.4.2. *From mathematical theorem to practical computational scheme: Kohn-Sham approach*

A major breakthrough that paved the way for practical implementation of DFT is the approach devised by Kohn and Sham (KS) [42]. They addressed the above (Section 2.4.1) problem using *independent particles* that had *interacting electronic densities.* KS's approach *assumed* that the ground state density of the interacting many-body system can be viewed as an independent electron residing in single electron wave functions, and all the effects of the exchange and correlations that arise due to the indistinguishability of electrons can be grouped into an *exchange-correlation functional* of the electronic density. Since the operator expressions for the kinetic and classical electrostatic energies are known, we can derive the energies from the orbitals of the independent particles, and the exchange-correlation part is in principle determined by the exchange-correlation functional. Thus, the KS expression for energy N-electron system can be written as:

$$E_{KS} = T_{ind}[n]+E_{hartree}[n] +\int d^3rV_{ex}(r)n(r)+E_{II}+E_{xc}(n) \quad (5)$$

$$n(r) = \sum_{i=1}^{N}|\psi_i|^2 \quad (6)$$

where, $T_{ind}[n] = \sum_i \langle\psi_i|\hat{T}|\psi_i\rangle$; $E_{hartree} = \frac{1}{2}\int\frac{d^3rd^3r'n(r)n(r')}{|r-r'|}$; E_{xc} = Exchange-correlation energy functional.

Comparing the HK and KS expressions for energies, the exchange-correlation energy $E_{xc}(n) = \left\langle\hat{T}\right\rangle-\left\langle\hat{T}_{ind}\right\rangle+\left\langle\hat{V}\right\rangle-\left\langle\hat{E}_{hartree}\right\rangle$, is the difference between the total kinetic and potential energies of the interacting many-electron system and kinetic and potential energies computed using the independent particles. Since the long-range Hartree interactions and kinetic energies have been subtracted, this offers a possibility of expressing the exchange-correlation function as a local/gradient corrected functional of density. Hence, the exchange-correlation functional can be written as:

$$E_{xc}[n]=\int drn(r)\varepsilon_{xc}(r,[n]) \quad (7)$$

where, $\varepsilon_{xc}(r,[n])$ is the exchange-correlation energy per electron at $\mathbf{r}$ depending on local electronic density $n(r)$.

To obtain the ground state energy, the KS energy expression (eq. 5) can be minimized by varying the electron density, which effectively changes the average potential felt by each electron in its orbital. This method leads to the KS equations that can be written as:

$$(H_{KS}(r)-\varepsilon_i)\psi_i(r)=0 \quad (8)$$

where, $H_{KS}(r) = -\frac{1}{2}\nabla^2 + V_{KS}(r)$; $V_{KS}(r) = V_{ex}(r) + \frac{\delta E_{hartree}}{\delta n(r)} + \frac{\delta E_{xc}}{\delta n(r)}$; $V_{KS}(r) = V_{ex}(r)+ V_{hartree}(r)+V_{xc}(r)$.

These equations are solved self-consistently to obtain the orbital by calculating the KS potential ($V_{KS}(r)$) and would lead to the correct ground state if an exact expression for exchange correlation functional is available. Also, by the HK theorem, there should be an unique KS potential corresponding to a particular electron density.

It should be noted that KS orbitals are mathematical objects that are used to build the correct electronic density and hence, KS orbitals do not have any physical significance. However, studies have shown that the symmetries, shape and ordering of energies of the KS orbitals are similar to the orbitals obtained from extended Huckel calculations. This analogy is very important because extended Huckel molecular orbital calculations are closely connected to ideas of chemical reactivity obtained from qualitative molecular orbital theories (QMOT) [39]. Hence, many of the intuitive ideas of chemical reactivity/QMOT are consistent with orbitals obtained from DFT [44].

There are many flavors of DFT and WFT in terms of accuracy and approximations, but a general rule is that greater accuracy requires

greater computational time and hence, smaller the size of the system that can be studied with that computational method [35]. However, for obtaining results of given accuracy in a given system, DFT is less computationally intensive in comparison to WFT, and hence, most of the quantum chemical computational studies relevant to heterogeneous catalysis have been performed using DFT [34,35].

2.5. *Current shortcomings of DFT*

In the context of heterogeneous catalysis, it is important to be informed about two shortcomings of DFT, namely, self-interaction error and electronic spin related issues, both of which are most critical in the context of heterogeneous oxidation reactions using metal oxides as catalysts [30,42,45,46]. DFT, as opposed to WFT, has self-interaction error because the self-interaction of the electrons is not cancelled by the exchange integrals. Such errors become important in oxidation reactions, which involve creation of oxygen vacancies from the oxide/doped oxide surfaces [45], and DFT does not give correct energetics in this case. Further, as DFT does not provide a wave function, properties like spin cannot be properly defined. It is well known from quantum theory that spin should be conserved during the course of the reaction for the reaction rate to be high [30,46]. Currently, the method to enforce such conditions within the framework of DFT is not clear. This is an important issue because O_2 molecule is a triplet and many important active sites in an oxide surface are spin-polarized, and hence, formal methods have to be developed to treat them within DFT. These issues are elaborated in greater detail in a variety of articles [45,46].

2.6. *Practical aspects of DFT simulations in catalysis*

Beyond WFT and DFT, practical electronic structure simulations involve knowledge of basis set, pseudopotentials, concepts from band structure and group theory, numerical methods and parallel computing and these are discussed in a number of textbooks [35,42,43].

Most of the computational research groups that are involved in the modeling and design of heterogeneous catalysts do not develop a code from scratch in their own group. Due to a variety of historical, cultural, technical and non-technical reasons (like user-friendliness), certain programs have become more popular. As most of these programs provide access to the source code, it is possible to modify certain parts of the program if the need arises. Currently, in the area of heterogeneous catalysts, some of the codes that are being used extensively are Dacapo, PWSCF, Abinit, SIESTA, CPMD, VASP, CRYSTAL, CASTEP and DMOL, of which the first five are open source codes. Most of these codes come with good references, tutorials and mailing lists to get a well-motivated novice started.

While the above discussion has focused mainly on methods to obtain the energetics of a reaction, which is the most important factor in computational catalytic discovery, a variety of methods like kinetic Monte-Carlo simulations exist for simulating kinetics and are used in conjunction with DFT calculations [35,47].

A typical computational study in heterogeneous catalysis proceeds in the following manner: 1) Total energy of the surface is minimized. This step involves an iterative calculation of electronic energy at a given nuclear geometry, followed by movement of nuclear positions along the gradient in energy, which is followed by another electronic minimization and so on till the total energy reaches a minimum. 2) The reactant is then adsorbed on to the surface to obtain the energy minima of the system comprising of reactant bound to the surface. 3) The products of the reaction are guessed and are bound to the surface, following which another energy minimization is performed. 4) Knowledge of the reactant geometry on the surface and product geometry on the surface paves way to a variety of methods to compute the transition state and hence, obtain the activation energy for the reaction [35].

3. Density functional theory as a design tool in catalysis

The approach of designing catalysts using DFT has been pioneered by the group of Norksov and brought to fruition by them and other groups. The central concepts involved in this approach are discussed in this section.

3.1. *Reactivity descriptors and Bronsted–Evan–Polanyi relationships*

In certain catalytic systems like CO oxidation on Ru surface, it is possible to explore all possible reaction pathways in great detail using DFT [47]. Having computed all the energetics of different possibilities, this information is fed to computational methods like kinetic Monte Carlo simulations to obtain *ab-initio* statistical mechanical kinetic rate data. While a detailed understanding is possible from such an analysis, this approach has been adopted only for few systems as the number of computations involved is enormous.

Another approach that has been more successful in terms of finding new catalytic systems starts with the identification of the reactivity descriptor [34]. In many cases, identification of the reactivity descriptor for a simple catalytic system involves a prediction

Figure 2: Mars and Van Krevelen mechanism for heterogeneous catalytic oxidation reactions and first proposed for oxidation in V_2O_5. The oxygen that is needed for oxidizing reactant R-R' is obtained from the oxide lattice (indicated by L) and is accompanied by the creation of surface oxygen vacancy. Dotted lines indicate bond formation between the oxygen from the oxide surface and the adsorbed reductant. To complete the catalytic cycle, the surface oxygen vacancy has to be healed by oxygen from the gas phase.

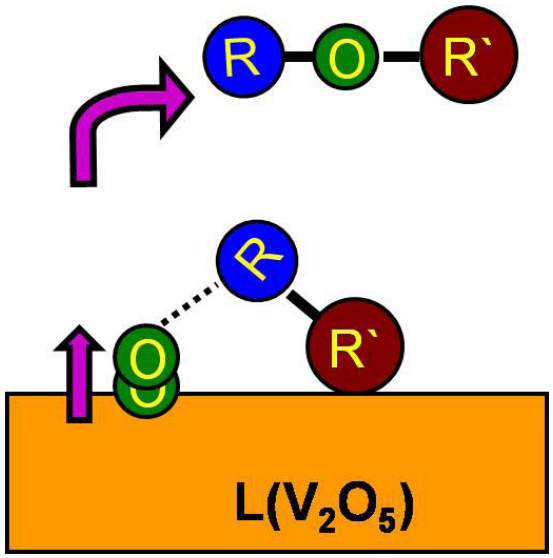

based on previous experimental/computational chemical information and an understanding of chemical reactivity. For e.g., N_2 dissociation is the reactivity descriptor for ammonia synthesis, CO dissociation for methanation, O_2 dissociation for a fuel cell cathodic oxygen reduction and H_2 dissociation for fuel cell anodic oxidation. In general, these choices are in accordance with our intuitive notions on chemical reactivity. Once the reactivity descriptor has been identified, the energetics of this reaction step is computed over a range of catalytic surfaces (currently, usually metallic alloys).

The best catalyst for a reaction is decided on the basis of Sabatier's principle [34,35], which is most easily explained with a specific example. Let us consider that we are looking for a catalyst for NH_3 synthesis, where N_2 bond breaking is the reactivity descriptor. In general, the activation barrier for bond breaking on a particular surface scales linearly with the adsorption energies on that surface. This scaling is called the Bronsted–Evans–Polanyi (BEP) relationship [34,35], and this empirical principle has existed from the early days of physical organic chemistry. In keeping with the BEP relationship, to decrease the activation barrier for N_2 dissociation, we need to have surfaces that adsorb N_2 (and N) very well. However, if N_2 adsorbs very well, it may also be anticipated (and this is observed to be true) that the reaction intermediates like NH and NH_2 also adsorb well, which makes desorption of the product (gas phase NH_3) difficult. Therefore, a delicate balance needs to be achieved to make the surface a good catalyst: the surface should adsorb well to decrease the activation energy of N_2 dissociation, but not so strongly that it will make desorption of the products difficult. This delicate balance required for a surface to act as a good catalyst is the crux of the Sabatier principle.

We mentioned that the activation energy of N_2 dissociation decreases when the surface adsorbs N atom better and that this scaling is linear. Similar linear scaling has also been observed in other systems like CO dissociation where the activation energy decreases if C and O adsorb better on the surface [3,34,37]. Other interesting scaling relationships for molecules adsorbing on the surfaces have also been documented via DFT [34,36].

3.2. *Systems currently amenable to computational catalyst design*

Currently, most of the systems for which this approach has been fruitfully employed involve a single bond breaking step of a diatomic molecule [3,34,36]. While such systems appear to be very simplistic, many such systems are industrially important [3,34,36]. However, in the near future more complicated hydrocarbon reactions will certainly be studied.

Most of these systems have transition metal/alloy surfaces as catalysts [3,34,36]. Variants like near-surface alloys/core-shell alloy particles have also been considered [3,34,36]. Such catalytic metallic surfaces are advantageous from many points of view. Firstly, they are structurally simpler compared to oxides/sulfides because in these metal surfaces only the closed packed surfaces are most important in terms of stability and the problems of non-stoichiometry are not that critical. Secondly, DFT is much more accurate in handling metallic systems as compared to handling transition metal oxides (see Section 2.5). Moving away from metallic/alloy catalysts to other compounds like oxides/sulfides poses a much greater challenge in comparison to moving from diatomic molecules to molecules of greater complexities.

3.3. *Selectivity, multi-step reactions and electronic factors*

While the previous section discussed the principles behind designing a surface to increase the rate of a particular reaction, surfaces have also been designed for increasing selectivity [3,34,36]. The design principle for increasing selectivity is very

Figure 3: Cation subsitutional doping of Zn atom by Au dopant {indicated by D(Au)} in a ZnO lattice. Introduction of the Au dopant is expected to facilitate the removal of O_a from the doped ZnO lattice thereby making it a better Mars and Van Krevelen oxidant when compared to undoped ZnO surface.

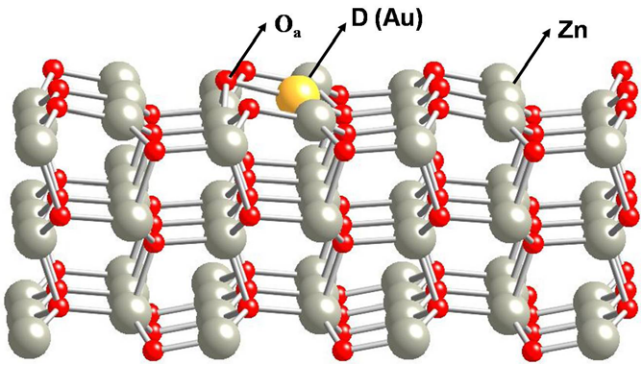

Figure 4: The position in the periodic table of various dopants in ZnO surface. The value of SOVFE (in eV) is indicated in each box for the doped oxide (for example, the SOVFE for Ti doped ZnO is 5.5 eV). The dopants in red boxes decrease SOVFE, and dopants in the blue box increase SOVFE as compared to the SOVFE of undoped ZnO. Boxes with a line along the diagonal contain dopants that segregate at the surface. Adapted from *J. Phys. Chem. C.*, **111**, 8617 (2007).

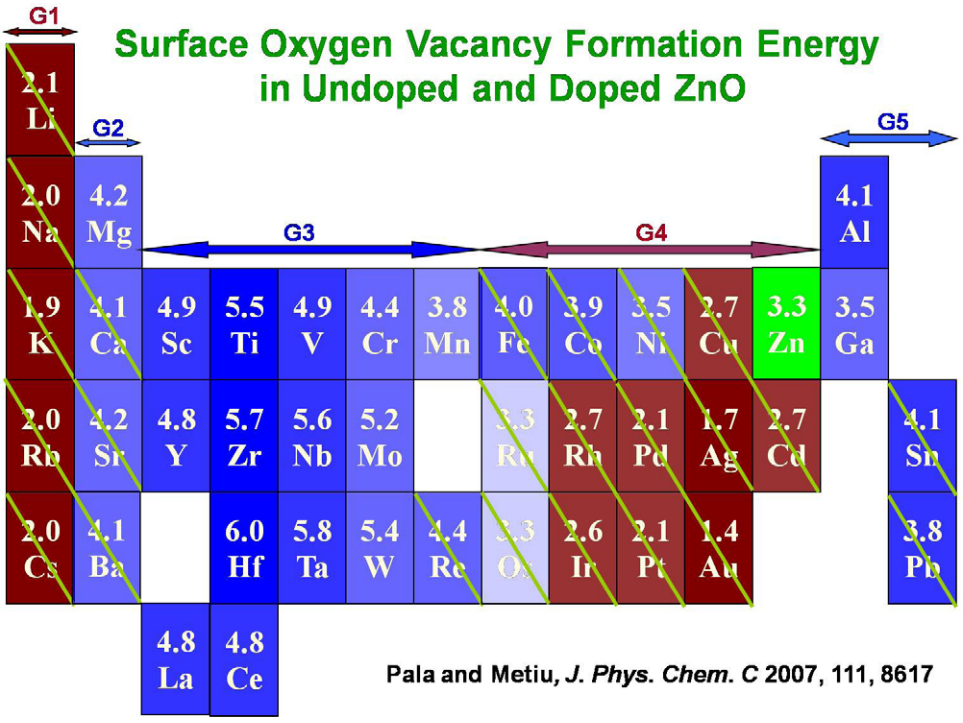

similar to the strategy for increasing rates, except that in the former, multiple reaction pathways exist, but only a single pathway needs to be optimally promoted [3,34,36]. Hence, the computational design strategy is to look for a surface where the rate of the desired reaction is the highest in comparison to the other undesired reaction pathways.

The Bronsted–Evan–Polanyi (BEP) relationships have been very useful in computational catalyst design [3,34,36] because they help in obtaining the activation barrier (which is harder to compute) from adsorption energies (which are easier to

Figure 5: Electronic charge distribution obtained from a DFT calculation of a Ti doped ZnO surface. Only a part of the surface is shown. Substitutional doping of a higher valent cation (like Ti) for Zn in a ZnO lattice results in an excess (in comparison to charge density around Zn in ZnO) electronic cloud, which can further bind to O_2 molecules from the gas phase. O_2 molecules thus activated may participate in non-Mars and Van Krevelen oxidation mechanism. Adapted from *J. Catal.* **254**, 325 (2008).

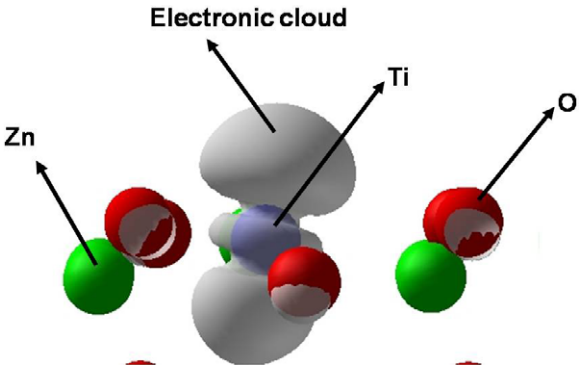

compute). The BEP relationships have also been extended to multi-step reactions [48]. In a reaction that has multiple steps, each of the individual steps obeys the BEP relationship. For e.g., for a reaction A→B→C→D, where B and C are reaction intermediates, the activation barrier for the reaction B→C depends on the energy difference between B and C.

To summarize, the above discussion clearly demonstrates that DFT provides a practical computational scheme for designing catalysts in certain classes of reactions [3,34,36]. Besides providing a practical computational method, DFT also provides insight into the underlying principles behind the variation in energies. The coupling of the electronic structure of the surface with the electronic states of the adsorbent is crucial for rationalizing the variation in energies. In the case of transition metal alloys, the "d-band" model has been utilized to rationalize energy variations [34,37]. In the "d-band" model, the position of the d-band relative to the Fermi level, and its coupling to the valence states of the adsorbing molecules determines the strength of the adsorption. Closer the center of the d-band is to the Fermi level, more of the anti-bonding orbitals formed due to adsorption will be empty and hence, higher is the strength of the chemisorption bond.

4. Computational design of doped oxide catalysts

Our research contributions on the design of computational using doped oxides was partly inspired by the successes of the approach pioneered by the group of Prof. Norskov, Technical University of Denmark and was an attempt to extend their strategy to systems other than transition metal alloy surfaces. Oxides offer additional complexities not present in metal surfaces. Unlike in a metal surface, in which the close-packed surface structure dominates as it is the most stable surface, it is not clear what surface of the metal oxide is most stable. Wulf construction to quantify the surface energies of different surfaces is complicated by the presence of polar surfaces and possible non-stoichiometric surfaces.

Heterogeneous catalytic oxidations are industrially very important [2,49], and it was felt that the strategies for designing catalysts should address this class of reactions. The natural choice of catalysts for this class of reaction is the oxides and doped oxides provided a starting point in terms of a simple functionalization to create active sites on the surface [5–33]. Further, excellent experimental work carried out by group of Prof. Hegde, Indian Institute of Science and others encouraged us to explore these systems computationally [5–25].

4.1. *Oxygen vacancy formation as a reactivity descriptor in heterogeneous catalytic oxidation reactions*

Heterogeneous catalytic oxidations are known to operate via the Mars and Van Krevelen (MVK) mechanism [49,50]. In this mechanism, the oxygen that needs to be supplied for oxidizing the reactant comes from a metal oxide surface and is accompanied by the formation of a surface oxygen vacancy (Fig. 2). While it may seem that the surface oxygen vacancy formation energy (SOVFE) is a natural choice for a reactivity descriptor in heterogeneous catalytic oxidation, this choice is

Figure 6: A generic catalytic cycle via the non-Mars and Van Krevelen mechanism. In the top right figure, the adsorption energies of O_2 on various doped ZnO surface are shown. It is clearly seen that doping ZnO with V or Ti or Al makes the doped oxide adsorb O_2 exothermically. Mg and Na doped ZnO do not adsorb O_2. In step 2 (top left), one of the oxygen atoms (represented as 1/2 O_2) is removed from the adsorbed dioxygen molecule and this can be given to the reductant R. This step can be followed by adsorbing one more O_2 molecule from the gas phase to form an ozone-like complex on the doped oxide surface (bottom center). The energy for this step indicates that this scenario is possible in ZnO doped with V, Ti, Al and Mg but not in Na doped ZnO. To complete the catalytic cycle, one of the oxygen atoms from the ozone-like complex can be removed to form a dioxygen adsorbed on the doped surface and the energetics of this process is also shown.

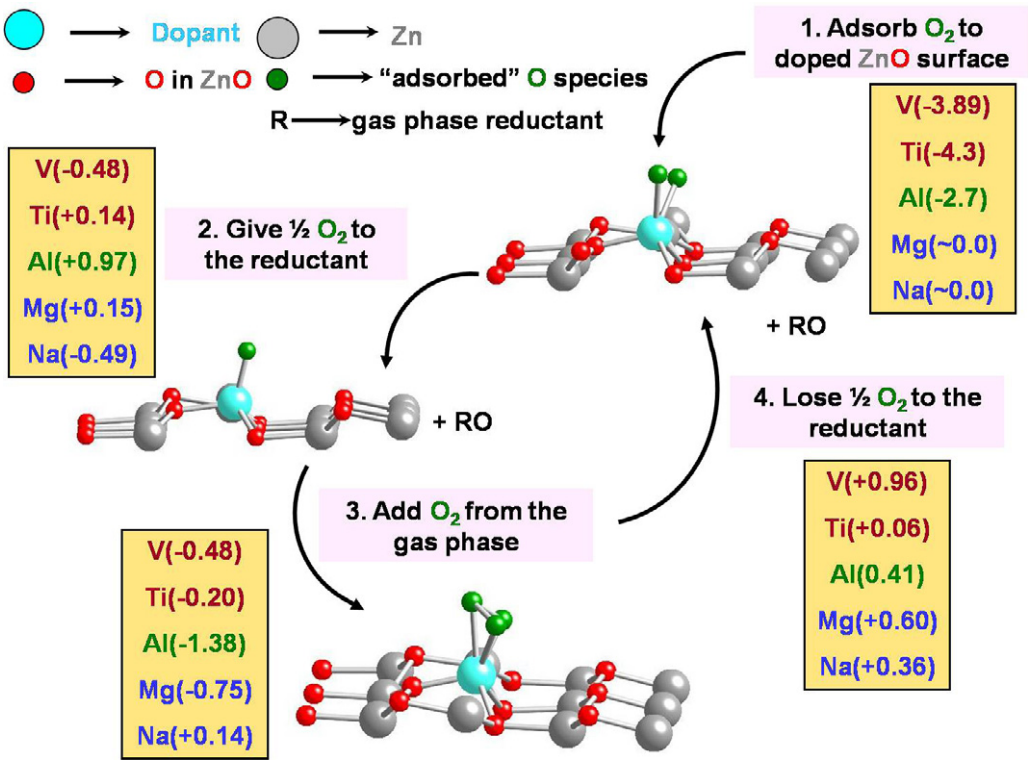

qualitatively different from the reactivity descriptors utilized for previous efforts in computational catalyst design. All the previous efforts involved the energetics of an elementary step, such as the energy for bond breaking of a diatomic molecule. It is almost certain that the surface oxygen vacancy formation is not an elementary step. In the absence of a generic elementary step for characterizing heterogeneous catalytic oxidation, SOVFE seemed to be the only choice for a reactivity descriptor.

Many experiments suggested that substitutional doping by a cation (Fig. 3) of the oxides decreases the SOVFE and renders the oxide a better oxidant. However, it was not clear what factors governed the changes in SOVFE and hence, a comprehensive study on how SOVFE changed with different dopants was undertaken (Fig. 4). While many doped oxides experiments have been performed using ceria and titania as the host oxide, our choice of the host oxide, ZnO, was partly governed by the feasibility of undertaking experiments that were planned in collaboration with the research group of Prof. Eric McFarland at the University of California, Santa Barbara. The other important reason for employing ZnO as a host oxide was that it was possible to dope ZnO with a range of dopants that had higher valency than the cation of the host oxide, which would not have been possible with ceria/titania.

The calculations showed that primarily the alkali dopants, Ag and Au weakened the bond of surface oxygen to the oxide [27]. All other dopants either cause a small change in SOVFE or considerably strengthen the bond between surface oxygen and the oxide. It could be inferred that those dopants that increased SOVFE would not be better Mars–van Krevelen oxidants as compared to undoped ZnO. More importantly, this extensive computational study raised the possibility that a dopant with high "formal charge/valence" (e.g., Ti, Al, Ce, V, Nb, etc.) is substantially under-coordinated when it replaces

Figure 7: (a) A schematic illustrating dopant induced non-Mars and Van Krevelen oxidation mechanism in which two CO molecules are oxidized to two CO_2 molecules using a molecule of O_2 in a CO rich atmosphere. The zero level for this reaction energy diagram is with oxygen and two CO molecules in the gas phase and the doped ZnO surface is uncoordinated to any reactant/reaction intermediate. The brown (blue) lines indicate the energy of the reaction intermediates for Ti doped ZnO (Al doped ZnO). The first step is adsorption of dioxygen from the gas phase on to the doped oxide (For e.g., -3.8 eV refers to the adsorption energy of O_2 on to Ti doped ZnO). The second step is adsorption of CO on to adsorbed dioxygen (For e.g., in Ti doped ZnO, CO adsorbs on to the adsorbed dioxygen with an adsorption energy of -4.1 eV, and the energy of the carbonate adsorbed on to Ti doped ZnO will be -7.9 eV). The third step is dissociation of the carbonate into gas phase CO_2 leaving O adatom on the dopant. The fourth step is CO_2 adsorbed on to the dopant. The final step is desorption of CO_2 to the gas phase. The energy of reaction of CO (g) + 2 O_2 (g) $\rightarrow$ CO_2 (g) is -6.6 eV. Adapted from *J. Catal.* **266**, 50 (2009).

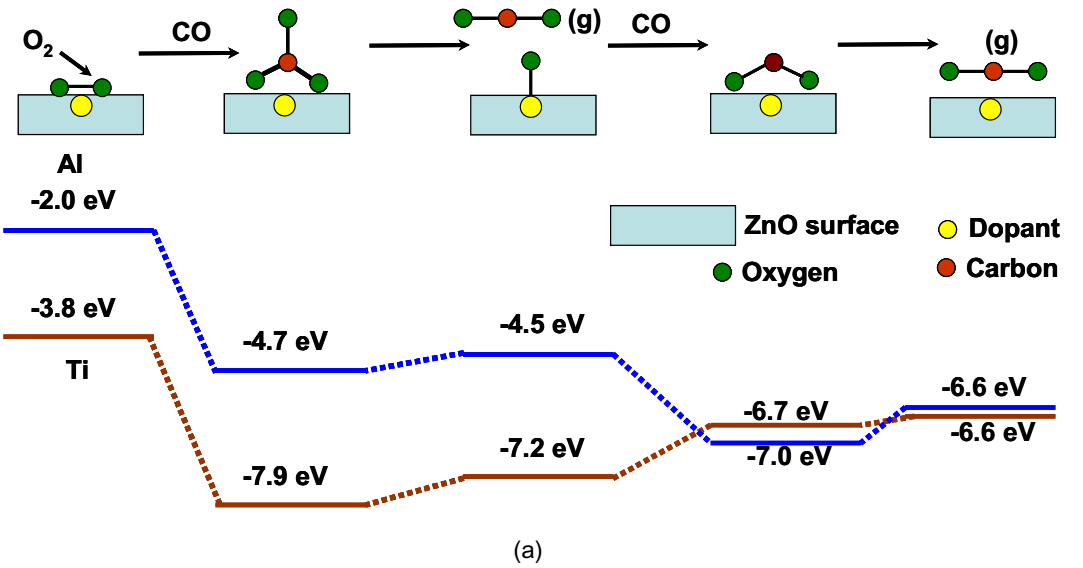

(a)

a Zn atom in the ZnO lattice. Thus, it may adsorb and activate a gas-phase O_2 molecule, which may then participate in the oxidation reaction, which is in contrast to the traditional paradigm of the Mars and Van Krevelen mechanism.

4.2. *Non–Mars Van Krevelen mechanism*

When a higher "valent" dopant like Ti or Al substitutes some Zn atoms in ZnO, the excess electronic density is concentrated on the dopant (Fig. 5). This electronic density can be utilized for adsorbing and activating O_2, which may then participate in an oxidation reaction [29]. Such a mechanism (referred to as non-MVK mechanism in this review) does not necessitate the creation of surface oxygen vacancies. As preliminary computational investigations (Fig. 6) showed promise, more detailed computational studies were conducted for CO oxidation reaction, which is a good test reaction for calibrating oxidation activity. The computational studies involved only the energetics of the reaction intermediates and activation energies were not computed for all the steps [29]. While this may give an indication of the minimum activation energies in certain instances, one cannot say much about the rates or overall activity. To obtain a more conclusive statement about the rates, activation energies have to be computed, which is very computationally demanding.

As a variety of catalytic cycles pointed towards the plausibility of the non-MVK mechanism (Fig. 7), experiments were performed to test the proposed non-MVK catalyst "design" principle [29]. The rationale behind the design principle was that if only the MVK mechanism contributed to oxidation activity, then Ti (or Al) doped ZnO would be less effective catalysts than undoped ZnO as Ti (or Al) doping made it *more difficult to create surface oxygen vacancies*. If a non-MVK mechanism contributed to oxidation activity, it may be possible that Ti (or Al) doped ZnO would be better oxidation catalysts than undoped ZnO. This non-MVK mechanism, which was proposed based on computations, was clearly supported by experiments wherein Ti (or Al) doped ZnO were demonstrated to exhibit better oxidation catalytic activity (measured in terms of light-off temperature) as compared to undoped ZnO. As

Figure 7: (b) A schematic illustrating dopant induced non-Mars and Van Krevelen oxidation mechanism in which two CO molecules are oxidized to two CO_2 molecules using a molecule of O_2 in an O_2 rich atmosphere, where an ozone-like reaction intermediate can be formed. The zero level for this reaction energy diagram is the same as in Fig. 7 (a). Adapted from *J. Catal.* **266**, 50 (2009).

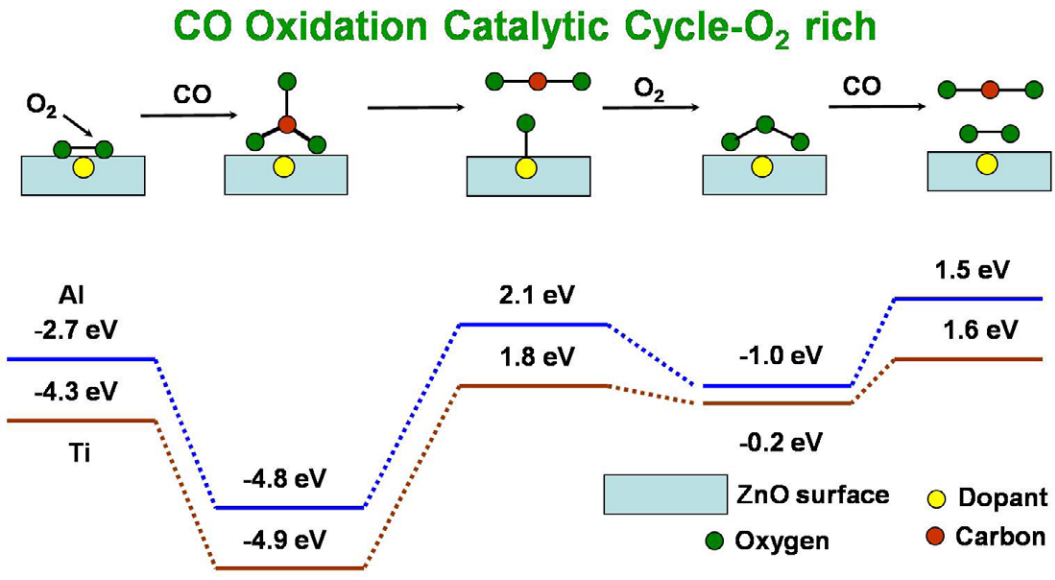

(b)

the utility of simulation in a fairly complex oxide catalyst was clearly proven, we decided to investigate the mechanism further by isotope experiments.

Historically, isotope experiments have played a valuable (albeit expensive) role in unraveling mechanisms in heterogeneous catalysis [49]. In fact, support for the traditional MVK mechanism was also derived from isotope experiments [49]. For example, in a catalytic oxidation experiment using an oxide, if $^{18}O_2$ and $C^{16}O$ are supplied in the gas phase, then the presence of only $C^{16}O_2$ in the initial product stream suggests that the oxygen for oxidation comes from the surface (assuming that the metal oxide does not contain any ^{18}O). The analysis of later stages of product evolution may be complicated from the fact that $^{18}O_2$ might get incorporated into the surface at a later point in time.

In the context of non-MVK mechanism, supplying $^{18}O_2$ and $C^{16}O$ should result only in the formation of $^{18}OC^{16}O$, which would have supported the simulations in totality. However, while the product stream had $^{18}OC^{16}O$, it also had significant amount of $^{16}OC^{16}O$ and little bit of $^{18}OC^{18}O$ (Fig. 8): both of which were not supported by the analysis performed via simulations. But having the experimental results at hand [29], it was possible to propose and computationally suggest another possibility. When the adsorbed oxygen on the higher valent dopant is consumed for oxidation by the reductant, the higher valent dopant picks up an oxygen atom from the surface and thereby creates an oxygen vacancy on the surface [29]. This may be called a "pseudo-MVK" mechanism (Fig. 9). This oxygen, now adsorbed on to the higher valent dopant can give rise to a $^{16}OC^{16}O$ product stream.

The experiments also exhibited an interesting hysteresis in oxidation activity and the physical underpinnings of this phenomenon are being currently investigated. Further, studies are being conducted to explore new design strategies using the non-MVK oxidation mechanism. In particular, it appears that breaking of the CH bond via the non-MVK mechanism will have much lower activation energy than if bond-breaking occurs via the traditional MVK mechanism. However, whether such a pathway can lead to a sustainable catalytic cycle has to be examined both experimentally and computationally.

4.3. *Selectivity and doping*

While there have been many studies on the effect of doping on the rate of a reaction, fewer studies have focused on how doping oxides affects selectivity. This question has been addressed for doped ZnO surfaces using methanol adsorption studies [28]. Methanol adsorption has been extensively studied experimentally to probe the nature of the active sites on the surface. In this study, the first bond

Figure 7: (c) A schematic illustrating dopant induced non-Mars and Van Krevelen oxidation mechanism in which two CO molecules are oxidized to two CO_2 molecules using a molecule of O_2 in an O_2 rich atmosphere via the formation of an oxalate reaction intermediate. The zero level for this reaction energy diagram is the same as in Fig. 7 (a). Adapted from *J. Catal.* **266**, 50 (2009).

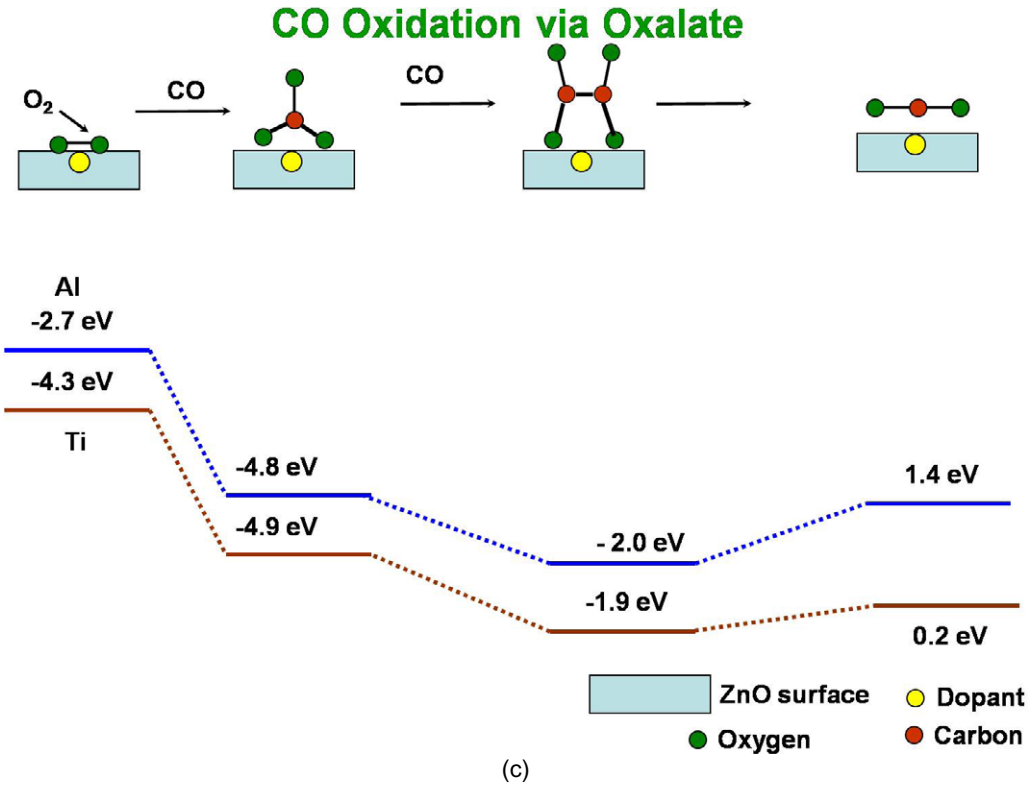

(c)

breaking step was analyzed and did not involve the entire catalytic cycle [28], the rationale being that the dissociation of different bonds will result in the formation of different end products. For e.g., if the CO bond of CH_3OH is broken, the possibility of forming an alkane product is greater than if the bond between CH and OH is broken in which case HCHO may be formed to a greater extent. Breaking the OH bond will promote the formation of di-methyl ether (Fig. 10). It was determined whether doping the surface of ZnO would change the propensity of the dissociative adsorption pathways. The results were encouraging (Fig. 10) and can be understood intuitively. For e.g., in the case of ZnO doped with Ti or Al, these dopants are under-coordinated and the energy will be lowered when they bind to oxygen. This results in the promotion of an adsorption mode that favors methoxy formation. Further, Ti or Al doped ZnO suppresses the dissociation of CH_3OH to formaldehyde. The opposite behavior is demonstrated by doping ZnO with alkali metal atoms like Na or K, wherein dissociation to formaldehyde is promoted. This is because doping ZnO with Na or K induces a hole on the surface oxygen atoms to which the alkali dopants are bound to and this makes the surface oxygen atoms abstract two H atoms from methanol. Further, the dissociation to methoxy is suppressed in alkali doped ZnO. Thus, as Ti or Al or Na or K promote certain dissociative adsorption modes and suppress certain other modes, these dopants increase the selectivity of specific dissociation products [28]. Certain other dopants (like Ag or Cu) do not increase selectivity as they do not greatly enhance a particular mode while inhibiting other dissociative adsorption modes.

4.4. *BEP relationships in doped oxide catalysts*

BEP linear relationships between activation energies and adsorption energies have been very fruitfully utilized to predict reaction rates on a variety of transition metal surfaces. As mentioned earlier, these relationships decrease the computational labor as obtaining activation energies are much more difficult in comparison to the computation of adsorption energies. It is desirable to demonstrate the existence of BEP relationships on catalytic surfaces more complex than transition metal alloys.

Figure 8: Oxygen isotope labeled experimental studies to test the non-MVK mechanism. While the presence of $^{18}OC^{16}O$ supports the non-MVK mechanism, the occurrence of $^{16}OC^{16}O$ and $C^{18}O_2$ suggests the participation of other mechanisms. These experimental results led to further computational studies and the hypothesis of "pseudo" MVK mechanism. Adapted from *J. Catal.* **266**, 50 (2009).

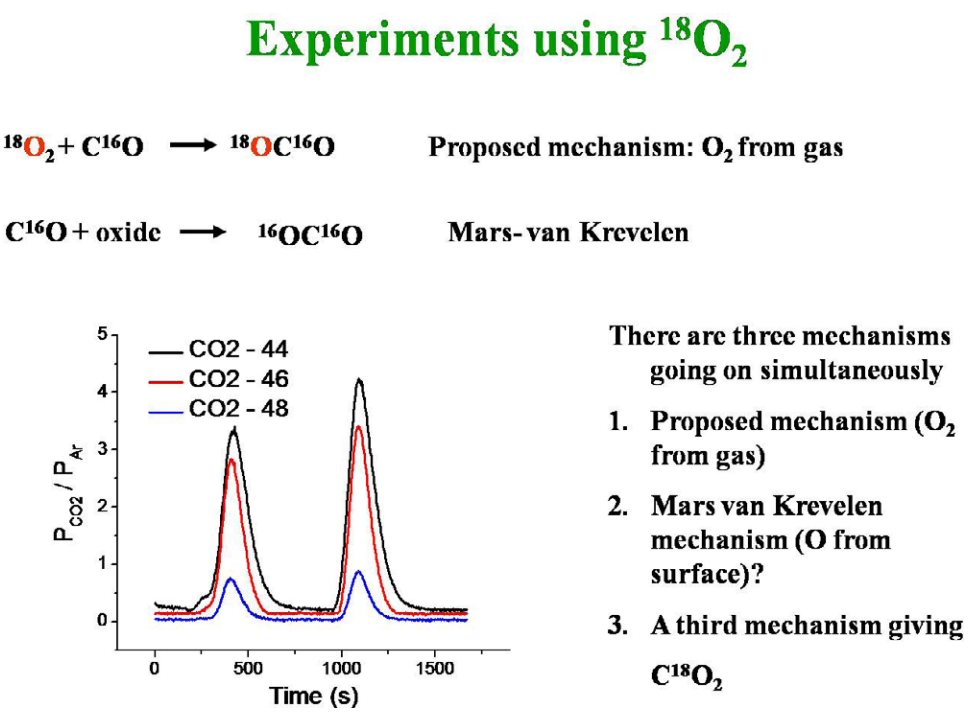

Figure 9: Schematic depicting "psuedo" MVK mechanism. When Ti doped ZnO surface does not have any O_2 adsorbed to Ti, a surface oxygen atom (indicated by green spheres) can be transferred on top of the dopant (this mechanism is referred to as the "pseudo"-MVK mechanism in the text). The initial position for the transferred oxygen atom is indicated by $\mathbf{O}_i$ and the final position of the transferred oxygen atom is indicated by $\mathbf{O}_f$. An approximate trajectory for the transferred oxygen atom is indicated by the block arrow and by a series of green spheres alongside the block arrow. This mechanism occurs only in Ti doped ZnO, and not for Al doped ZnO. Adapted from *J. Catal.* **266**, 50 (2009).

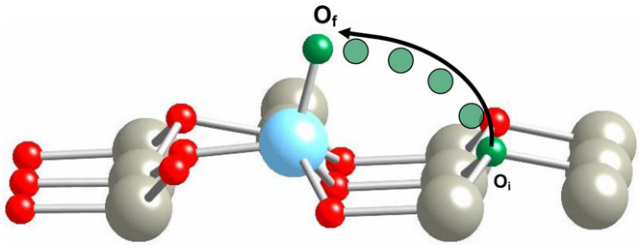

Such a study has been performed on doped TiO_2 surface [30]. The CO oxidation reaction scheme in doped TiO_2 surface is summarized in Fig. 11. DFT simulations (Fig. 12) show that the CO adsorption energy (step E1 in Fig. 11) and O_2 adsorption energy (step E3) is linearly related to surface oxygen vacancy formation energy (SOVFE). Like other BEP relationships, these can be anticipated intuitively. A greater SOVFE implies a stronger O bond to the surface and decreased tendency of O to adsorb CO in step E1. Additionally, higher the SOVFE, the greater will be the tendency of oxygen vacancy to adsorb O_2(step E3 in Fig 11). While such a scaling is expected for it to be linear is surprising.

Figure 10: Modulation of selectivity in dissociative adsorption of CH_3OH in doped ZnO. Three different dissociation pathways are explored here. In undoped ZnO, the adsorption energies of the methoxy (left) pathway is −0.7 eV, C–O bond dissociative pathway (middle) is −0.4 eV and HCHO formation pathway (right) is +1.6 eV. Ti or Al doped ZnO promote the methoxy pathway but suppress HCHO pathway. Na or K doped ZnO promote the HCHO pathway but suppress the methoxy pathway. Hence, the dopants Ti, Al, Na and K significantly change the selectivity, but other dopants studied here have marginal effects on selectivity. Adapted from *J. Catal.* **254**, 325 (2008).

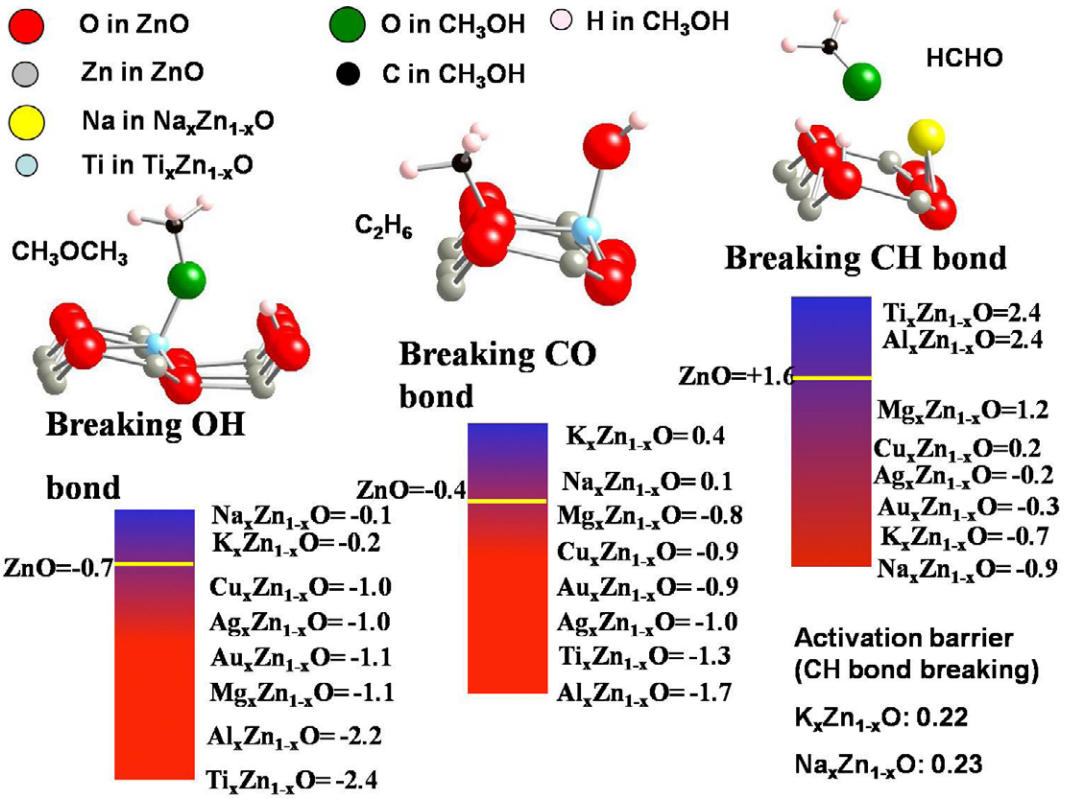

Conclusions and outlook

The motivation of this article is twofold: First, a general introduction to density functional theory (DFT) is provided along with a practical outlook on aspects of DFT that are more critical to computational catalyst design. Second, an overview is provided on the state of the art computational catalysts design. The case studies mentioned here suggest that computational catalyst design can be a successful strategy for transition metal alloy surfaces and especially if the reactants are simple diatomic molecules. The next few years are likely to strengthen the activity in these areas and increase the number of successful catalysts designed with the aid of DFT. The challenge lies in broadening the scope of computational catalyst design to include more complicated reactants and multi-component surfaces including oxides and sulfides. In electrochemical and photoelectrochemical systems, the aqueous medium also complicates the analysis and enriches the phenomenology. Preliminary computational catalyst design steps taken in this direction have been quite promising and much has been learnt from these calculations.

The main take-home message in the exercise of computational catalyst design employing doped oxides was not only in the unraveling of the non-MVK mechanism, but also in bringing out the importance of the close synergy between simulations and experiments. To some extent, a philosophy that has existed in computational catalyst design is that some factors (like energetics of reaction intermediates) are more easily computable and some other factors (like total rates) are more easily measurable. An optimal division of labor and utilization of a variety of experimental tools in conjunction with computer simulations is imperative for the discovery of new catalysts. Hence, for complex surfaces what may be more realistic is not a standalone approach to computational catalytic discovery, but an iterative exercise in which computations and experiments are coupled together to discover useful and interesting catalysts.

Figure 11: Schematic diagram of a single catalytic cycle for CO oxidation by doped TiO_2 catalysts. The yellow box indicates oxygen vacancy. The first reaction step is CO adsorption to the surface oxygen, the second step is CO_2 desorption, the third step is O_2 adsorption at the vacancy site, the fourth step is the reaction of the adsorbed O_2 with CO to form a carbonate and the fifth step is the decomposition of the carbonate to produce CO_2 and completion of the catalytic cycle. Adapted from *J. Phys. Chem. C,* **112**, 12398 (2008).

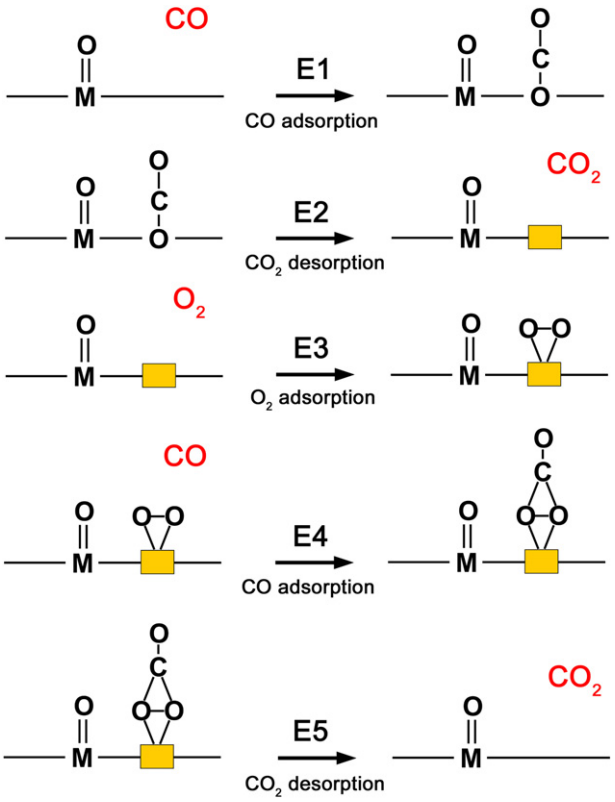

Figure 12: (a) A BEP like relationship between the energy of CO adsorption on the surface of the doped oxide and the energy of oxygen vacancy formation (b) The energy of oxygen adsorption at the oxygen vacancy site versus the energy of oxygen vacancy formation. Adapted from *J. Phys. Chem. C,* **112**, 12398 (2008).

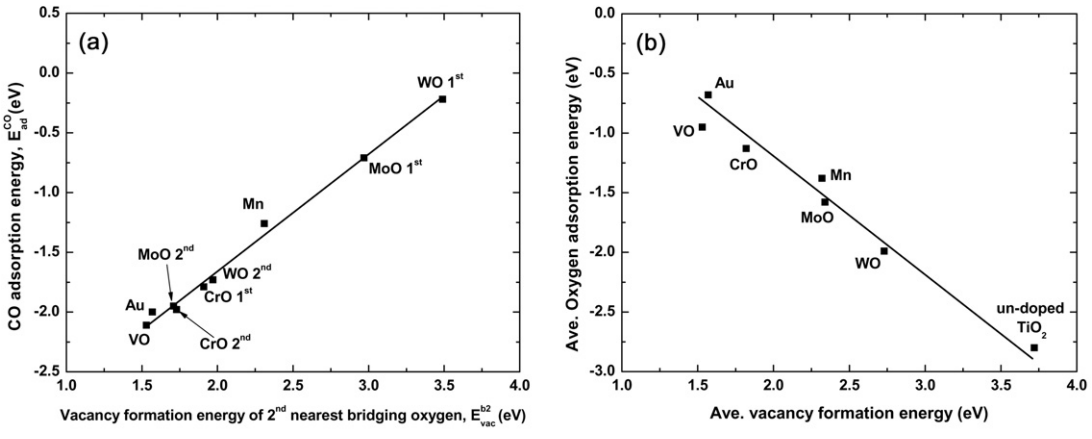

Acknowledgement

During the author's post doctoral fellowship at the University of California at Santa Barbara, the computational studies on doped oxide catalysts were conducted in collaboration with Prof. Horia Metiu and the experiments were conducted in collaboration with Prof. Eric McFarland. These research efforts were supported by the Air Force Office of Scientific Research and by the Partnership for International Research and Education at the University of California Santa Barbara, under a grant from the National Science Foundation.

Received 10 June 2010.

References

1. J. M. Thomas and W. J. Thomas. *Principles and Practice of Heterogeneous Catalysis*, Wiley-VCH.
2. C. H. Bartholomew and R. J. Farrauto. *Industrial catalytic processes*, John Wiley & Sons, 2006.
3. J. Greeley, J. K. Norskov, and M. Mavrikakis. Electronic structure and catalysis on metal surfaces. *Annual Review of Physical Chemistry* **53**: 319–348 (2002).
4. J. M. Thomas. Heterogeneous catalysis: Enigmas, illusions, challenges, realities, and emergent strategies of design. *Journal of Chemical Physics* **128**: (2008).
5. A. Cimino and F. S. Stone. Oxide solid solutions as catalysts, *Advances in catalysis*, Vol. 47, Advances in Catalysis, 2002, pp. 141–306.
6. T. Baidya, A. Gayen, M. S. Hegde, N. Ravishankar, and L. Dupont. Enhanced reducibility of Ce1-xTixO2 compared to that of CeO2 and higher redox catalytic activity of Ce1-x-yTixPtyO2-delta compared to that of Ce1-xPtxO2-delta. *J. Phys. Chem. B* **110**: 5262–5272 (2006).
7. P. Bera, S. Mitra, S. Sampath, and M. S. Hegde. Promoting effect of CeO2 in a Cu/CeO2 catalyst: lowering of redox potentials of Cu species in the CeO2 matrix. *Chem. Commun.* 927 (2001).
8. P. Bera, S. Malwadkar, A. Gayen, C. V. V. Satyanarayana, B. S. Rao, and M. S. Hegde. Low-temperature water gas shift reaction on combustion synthesized Ce1-xPtxO2-delta catalyst. *Catalysis Letters* **96**: 213–219 (2004).
9. P. Bera, A. Gayen, M. S. Hegde, N. P. Lalla, L. Spadaro, F. Frusteri, and F. Arena. Promoting effect of CeO2 in combustion synthesized Pt/CeO2 catalyst for CO oxidation. *Journal of Physical Chemistry B* **107**: 6122–6130 (2003).
10. P. Bera, K. R. Priolkar, A. Gayen, P. R. Sarode, M. S. Hegde, S. Emura, R. Kumashiro, V. Jayaram, and G. N. Subbanna. Ionic dispersion of Pt over CeO2 by the combustion method: Structural investigation by XRD, TEM, XPS, and EXAFS. *Chemistry of Materials* **15**: 2049–2060 (2003).
11. P. Bera, K. R. Priolkar, P. R. Sarode, M. S. Hegde, S. Emura, R. Kumashiro, and N. P. Lalla. Structural investigation of combustion synthesized Cu/CeO2 catalysts by EXAFS and other physical techniques: Formation of a Ce1-xCuxO2-delta solid solution. *Chemistry of Materials* **14**: 3591–3601 (2002).
12. K. Nagaveni, M. S. Hegde, and G. Madras. Structure and photocatalytic activity of Ti1-xMxO2 +/-delta (M = W, V, Ce, Zr, Fe, and Cu) synthesized by solution combustion method. *Journal of Physical Chemistry B* **108**: 20204–20212 (2004).
13. G. Dutta, U. V. Waghmare, T. Baidya, M. S. Hegde, K. R. Priolkar, and P. R. Sarode. Origin of enhanced reducibility/oxygen storage capacity of Ce1-xTixO2 compared to CeO2 or TiO2. *Chemistry of Materials* **18**: 3249–3256 (2006).
14. G. Dutta, U. V. Waghmare, T. Baidya, M. S. Hegde, K. R. Priolkar, and P. R. Sarode. Reducibility of Ce1-xZrxO2: origin of enhanced oxygen storage capacity. *Catalysis Letters* **108**: 165–172 (2006).
15. Y. Z. Chen, B. J. Liaw, and C. W. Huang. Selective oxidation of CO in excess hydrogen over CuO/CexSn1-xO2 catalysts. *Applied Catalysis a-General* **302**: 168–176 (2006).
16. Q. Fu, H. Saltsburg, and M. Flytzani-Stephanopoulos. Active nonmetallic Au and Pt species on ceria-based water-gas shift catalysts. *Science* **301**: 935–938 (2003).
17. G. J. Hutchings, M. S. Hall, A. F. Carley, P. Landon, B. E. Solsona, C. J. Kiely, A. Herzing, M. Makkee, J. A. Moulijn, A. Overweg, J. C. Fierro-Gonzalez, J. Guzman, and B. C. Gates. Role of gold cations in the oxidation of carbon monoxide catalyzed by iron oxide-supported gold. *Journal of Catalysis* **242**: 71–81 (2006).
18. Y. Nishihata, J. Mizuki, T. Akao, H. Tanaka, M. Uenishi, M. Kimura, T. Okamoto, and N. Hamada. Self-regeneration of a Pd-perovskite catalyst for automotive emissions control. *Nature* **418**: 164–167 (2002).
19. F. J. Perez-Alonso, I. Melian-Cabrera, M. L. Granados, F. Kapteijn, and J. L. G. Fierro. Synergy of FexCe1-xO2 mixed oxides for N2O decomposition. *Journal of Catalysis* **239**: 340–346 (2006).
20. S. Ricote, G. Jacobs, M. Milling, Y. Y. Ji, P. M. Patterson, and B. H. Davis. Low temperature water-gas shift: Characterization and testing of binary mixed oxides of ceria and zirconia promoted with Pt. *Applied Catalysis a-General* **303**: 35–47 (2006).
21. W. M. H. Sachtler, G. J. H. Dorgelo, J. Fahrenfort, and R. J. H. Voorhoeve. Correlation between catalytic and thermodynamic parameters of transition metal oxides, *Proceedings of the fourth international congress on catalysis*, 1968, pp. 454–465.
22. W. J. Shan, Z. C. Feng, Z. L. Li, Z. Jing, W. J. Shen, and L. Can. Oxidative steam reforming of methanol on Ce0.9Cu0.1OY catalysts prepared by deposition-precipitation, coprecipitation, and complexation-combustion methods. *Journal of Catalysis* **228**: 206–217 (2004).
23. A. M. Venezia, G. Pantaleo, A. Longo, G. Di Carlo, M. P. Casaletto, F. L. Liotta, and G. Deganello. Relationship between structure and CO oxidation activity of ceria-supported gold catalysts. *J. Phys. Chem. B* **109**: 2821–2827 (2005).
24. S. W. Wang, A. Y. Borisevich, S. N. Rashkeev, M. V. Glazoff, K. Sohlberg, S. J. Pennycook, and S. T. Pantelides. Dopants adsorbed as single atoms prevent degradation of catalysts. *Nature Materials* **3**: 143–146 (2004).
25. S. Zhao and R. J. Gorte. The effect of oxide dopants in ceria on n-butane oxidation. *Applied Catalysis a-General* **248**: 9–18 (2003).
26. S. Chretien and H. Metiu. Density functional study of the CO oxidation on a doped rutile TiO2(110): Effect of ionic Au in catalysis. *Catal. Lett.* **107**: 143–147 (2006).
27. R. G. S. Pala and H. Metiu. Modification of the oxidative power of ZnO(10(1)over-bar0) surface by substituting some surface Zn atoms with other metals. *Journal of Physical Chemistry C* **111**: 8617–8622 (2007).
28. R. G. S. Pala and H. Metiu. Selective promotion of different modes of methanol adsorption via the cation substitutional doping of a ZnO(10(1)over-bar0) surface. *Journal of Catalysis* **254**: 325–331 (2008).
29. R. G. S. Pala, W. Tang, M. M. Sushchikh, J. N. Park, A. J. Forman, G. Wu, A. Kleiman-Shwarsctein, J. P. Zhang, E. W. McFarland, and H. Metiu. CO oxidation by Ti- and Al-doped ZnO: Oxygen activation by adsorption on the dopant. *Journal of Catalysis* **266**: 50–58 (2009).
30. H. Y. Kim, H. M. Lee, R. G. S. Pala, V. Shapovalov, and H. Metiu. CO oxidation by rutile TiO2(110) doped with V, W, Cr, Mo, and Mn. *Journal of Physical Chemistry C* **112**: 12398–12408 (2008).
31. V. Shapovalov and H. Metiu. Catalysis by doped oxides: CO oxidation by AuxCe1-xO2. *J. Catal.* **245**: 205 (2007).
32. M. S. Palmer, M. Neurock, and M. M. Olken. Periodic density functional theory study of methane activation over La2O3: Activity of O2–, O–, O–2(2–), oxygen point defect, and Sr2+-

doped surface sites. *Journal of the American Chemical Society* **124**: 8452–8461 (2002).
33. M. A. Johnson, E. V. Stefanovich, and T. N. Truong. An ab initio study on the oxidative coupling of methane over a lithium-doped MgO catalyst: Surface defects and mechanism. *Journal of Physical Chemistry B* **101**: 3196–3201 (1997).
34. J. K. Norskov, T. Bligaard, J. Rossmeisl, and C. H. Christensen. Towards the computational design of solid catalysts. *Nature Chemistry* **1**: 37–46 (2009).
35. R. A. van Santen and M. Neurock. *Molecular Heterogeneous Catalysis: A Conceptual and Computational Approach* Wiley-VCH, 2006.
36. C. H. Christensen and J. K. Norskov. A molecular view of heterogeneous catalysis. *Journal of Chemical Physics* **128**: (2008).
37. B. Hammer and J. K. Norskov. Theoretical surface science and catalysis — calculations and concepts. *Advances in Catalysis* **45**: 71–129 (2000).
38. S. A. French, A. A. Sokol, S. T. Bromley, C. R. A. Catlow, S. C. Rogers, F. King, and P. Sherwood. From CO2 to methanol by hybrid QM/MM embedding. *Angewandte Chemie-International Edition* **40**: 4437–+ (2001).
39. R. Hoffmann. A Chemical and Theoretical Way to Look at Bonding on Surfaces. *Reviews of Modern Physics* **60**: 601–628 (1988).
40. J. Simons and J. Nochols. *Quantum Mechanics in Chemistry*, Oxford University Press, 1997.
41. T. P. Helgaker, J. P., and O. J. *Molecular Electronic-structure Theory*, John Wiley & Sons Inc, 2010.
42. R. M. Martin. *Electronic structure: Basic theory and practical methods*, Cambridge University Press, 2008.
43. M. Springborg. *Methods of Electronic-Structure Calculations: From Molecules to Solids*, Wiley, 2000.
44. R. Stowasser and R. Hoffmann. What do the Kohn–Sham orbitals and eigenvalues mean? *J. Am. Ceram. Soc.* **121**: 3414 (1999).
45. G. Pacchioni. Modeling doped and defective oxides in catalysis with density functional theory methods: Room for improvements. *Journal of Chemical Physics* **128**: (2008).
46. S. Chretien and H. Metiu. O-2 evolution on a clean partially reduced rutile TiO2(110) surface and on the same surface precovered with Au-1 and Au-2: The importance of spin conservation. *Journal of Chemical Physics* **129**: (2008).
47. K. Reuter and M. Scheffler. First-principles kinetic Monte Carlo simulations for heterogeneous catalysis: Application to the CO oxidation at RuO2(110). *Physical Review B* **73**: (2006).
48. D. Loffreda, F. Delbecq, F. Vigne, and P. Sautet. Fast Prediction of Selectivity in Heterogeneous Catalysis from Extended Bronsted–Evans–Polanyi Relations: A Theoretical Insight. *Angewandte Chemie-International Edition* **48**: 8978–8980 (2009).
49. A. Bielanski and J. Haber. *Oxygen in Catalysis*, CRC Press, 1990.
50. P. Mars and P. W. van Krevelen. *Chem. Eng Sci.* **3**: 41 (1954).

Raj Ganesh S. Pala works in the area of heterogeneous catalysis, electrochemical systems and photoelectrochemical methods for storing solar energy. The research focus of the group is on the elucidation of concepts that aid in designing functional materials that are useful in converting various forms of energy and also in reducing environmental pollution. Elucidation of these underlying principles often involves a semi-quantitative description of phenomena that span a wide range of length and time scales. In this context, analysis is made using a wide variety of computational and theoretical tools like quantum chemical density functional theory, molecular dynamics, lattice based Monte Carlo methods and continuum transport equations. These studies are closely work coupled with experiments performed in the group as a combined experimental and theoretical analysis is often imperative in addressing systems as complex as a typical industrial catalyst